THE JOURNAL OF PHYSICAL CHEMISTRY B

Article

pubs.acs.org/JPCB

Ab Initio Molecular Dynamics Study of the Mechanism of Proton Recombination with a Weak Base

Jérôme Cuny*[,†,‡] and Ali A. Hassanali*[,§]

[†]Laboratoire de Chimie et Physique Quantiques (LCPQ), Université de Toulouse III [UPS] and CNRS, 118 Route de Narbonne, F-31062 Toulouse, France

[‡]Department of Chemistry and Applied Biosciences, Eidgenössische Technische Hochschule Zürich and Università della Svizzera Italiana, CH-6900 Lugano, Switzerland

[§]Condensed Matter Physics Section, The Abdus Salaam International Center for Theoretical Physics, Strada Costiera 11, Trieste I-34151, Italy

Supporting Information

ABSTRACT: Despite its fundamental nature, many of the microscopic features of acid−base recombination remain poorly understood. In this work, we use ab initio molecular dynamics simulations to study the recombination of the proton with a weak base, the carbonate ion CO_3^{2-}. Our simulations elucidate the network structure around CO_3^{2-} that provides a distribution of pathways over which recombination can occur. We observe that the penultimate neutralization step involves a correlated behavior of the transferred protons that is mediated by the water wires decorating the carbonate. These concerted proton transfers are coupled to collective compressions of these water wires. We show further that these processes are dynamically coupled to the reorganization of the water molecules hydrating the CO_3^{2-} ion. The insights from these simulations help to bridge the structural and dynamical complexity of the microscopic mechanisms with those of phenomenological models invoked by experiments in this field.

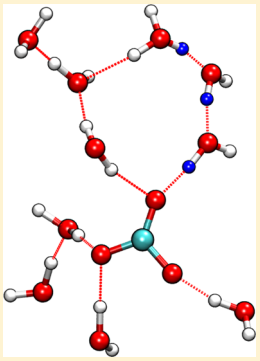

INTRODUCTION

Acid−base chemistry plays a key role in the biological activity of living organisms[1−3] as well as in the development of economical and efficient energy conversion processes of biomass into biofuels.[4] However, due to their underlying complexity, the related physicochemical mechanisms have been rationalized mostly in terms of phenomenological models, and few atomistic scale descriptions have been proposed. One of the critical steps in acid−base chemistry involves the transfer of protons through the hydrogen-bond network of the medium, and significant progress has been made in understanding this important process. This has been achieved mainly by use of ab initio molecular dynamics (AIMD) simulations and force-field approaches based on the multistate empirical valence bond formalism that have provided a wealth of information about the hydration structure of the proton and its dynamical behavior.[5−14] The picture that has emerged is that the proton migrates via structural diffusion through pathways in the hydrogen-bond network, a process commonly referred to as the Grotthuss mechanism,[15] which has been shown to involve a hierarchy of both spatial and temporal scales.[9,16] In contrast, the molecular mechanisms associated with the recombination of the proton and a base, as well as the thermodynamic and kinetic factors that control this process, have received much less attention in the literature.

Historically, the acid−base recombination mechanism has been mostly rationalized through the Eigen[17,18] and Weller[19−21] phenomenological kinetic model. Within this picture, the recombination occurs in two steps. In the initial diffusive regime, the proton moves freely in solution without any influence of the associated base. When reaching a critical distance (also referred to as contact distance) of ∼6 Å,[22] a reactive complex is formed (an example of such a reactive complex is presented in Figure 1 in the case of the carbonate ion) that subsequently leads to the protonation of the base. This is referred to as the recombination stage. Although the existence of these two main regimes is fairly well-accepted, over the past decade, several groups have attempted to refine this model by performing new and more elaborate experimental measurements.[23−35] For example, by photoinducing the initial ejection of a proton from a photoacid and by using time-resolved IR spectroscopy, Pines and co-workers have followed the neutralization of various bases such as acetate, chloroacetates, and bicarbonate.[23−28,31] These studies and others have identified factors that strongly affect the recombination stage, including, but not limited to, the chemical nature of the base, the concentration of both the photoacid and the base, the temperature, and, finally, the local structure of the reactive complex. However, despite the high-resolution techniques that were employed, the fast time scale of this regime (from the subpicosecond to several picoseconds) has so far prevented a clear atomistic scale description of the involved dynamical

Received: July 20, 2014
Revised: November 9, 2014
Published: November 21, 2014

dx.doi.org/10.1021/jp507246e | J. Phys. Chem. B 2014, 118, 13903−13912

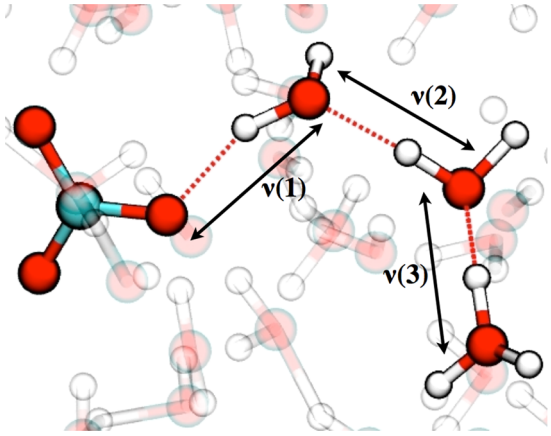

Figure 1. Example of the structure of a reactive complex appearing during the recombination stage of a base: here, the CO_3^{2-} ion with a proton. The complex is formed by CO_3^{2-} and H_3O^+ linked together by a water wire. The atoms belonging to the reactive complex are represented by opaque spheres, whereas the solvent water molecules are transparent. The hydrogen bonds along the water wire are represented by dotted lines, and the three proton transfer coordinates are indicated by black arrows.

activities and thus several models have been proposed. One such model is the three-stage mechanism proposed by Rini et al. in which the aforementioned recombination stage is subdivided in two: the encounter stage and the reactive stage.[24] In the former, when acid and base encounter, they form a loose complex characterized by a time constant of several picoseconds. In the latter, following some internal reorganization through a stepwise Grotthus mechanism,[15,36,37] the loose complex then transforms to a reactive tight complex that leads to proton transfer (PT) on the subpicosecond time scale. Note that in this model the conversion from loose to reactive complex has been proposed to involve reorganizations via sequential PTs. On the other hand, Cox et al. have interpreted some of their experimental data, which show a decrease in the recombination rate of acetate beyond a certain temperature, as indicating the presence of concerted PT processes.[33] Indeed, since concerted proton hopping is believed to occur through water wires, at high temperatures, the disruption of these wires inhibits this type of hopping mechanism.

Recently, Hassanali et al. have examined the recombination of the hydronium and hydroxide ions by use of AIMD simulations.[38] In these studies, they observed that at contact distance the ions are always bridged by a water wire composed of two water molecules. For the recombination to proceed, this wire has to undergo a collective compression that results in a concerted motion of three protons, leading to neutralization. This structural change of the wire is reminiscent of the reconstruction from loose to tight complex proposed by Rini et al. However, in the case of water's constituent ions, the recombination is dominated by concerted proton hopping, and it is a tightening of the wire through a compression mode that facilitates the process. The hydronium and hydroxide ions studied by Hassanali et al. represent a strong acid and base, respectively, and hence the question remains as to whether the observed behavior is transferable to other acid–base systems, for example, weaker Brønsted bases such as acetate or carbonate.

In this work, we use ab initio molecular dynamics to examine the recombination mechanism associated with the proton and the CO_3^{2-} ion. The versatility of AIMD simulations allows us to probe molecular details that have been very difficult to resolve experimentally. In particular, we show the existence of the loose complex proposed by Rini et al., but we demonstrate that neutralization does not necessarily evolve exclusively through a sequential stepwise proton transfer mechanism. Rather, concerted proton transfer events can also occur mediated by a different type of tight complex involving the existence of directed water wires linking the carbonate and the proton and their ability to undergo collective compressions. The reorganization of the solvation shell around the base is also coupled to this process. Furthermore, by performing our simulations at ambient and higher temperatures, we show that the concerted mechanism, within the limits of our theoretical approximations, still holds. Our studies also allow us to compare and contrast the recombination mechanisms in strong and weak bases, which are likely to be important for understanding acid–base chemistry in other chemical systems.

COMPUTATIONAL DETAILS

Recombination Trajectories. To generate the recombination trajectories, we initially performed two independent simulations of bulk water at 500 K using the TIP4P potential.[39] At the end of the runs, the CO_3^{2-} ion and the proton were inserted into the unit cells by deleting close contacts with nearby water molecules and ensuring that the ions were separated by ∼6.0 Å. AIMD simulations were then started from these two structures at 500 K to allow for an efficient equilibration while constraining the three O–H distances of H_3O^+ at 0.98 Å to avoid any recombination event. We also restrained the distance between the carbon of the carbonate and the oxygen of the hydronium to be ∼6.5 Å by applying a harmonic potential to avoid the formation of a contact ion pair. Subsequently, we decreased the simulation temperature to 400 K and then to 300 K while maintaining the aforementioned constrains. For the first set of simulations, the system was equilibrated during 19 and 14 ps at 300 and 400 K, respectively. We then performed 30 ps of simulation in the canonical ensemble at both temperatures, from which we uniformly sampled initial conditions to further propagate unconstrained microcanonical dynamics of length 2 ps each. In the ensuing discussion, we present only the recombination mechanism obtained from this first set of simulations for which, among the 100 and 75 energy-conserving simulations that we performed at 300 and 400 K, recombination occurs along 35 and 26 of them, respectively. All of the data presented in this article are extracted from these energy-conserving simulations only. In the Supporting Information, the simulation details of the second set of simulations are provided as well as the results that we obtained from them.

AIMD Simulation Parameters. All of the AIMD simulations consisted of a 12.459 Å cubic box containing 62 water molecules, one proton, and one carbonate ion. The simulations were performed using the Car–Parrinello approach as implemented in the CPMD code.[40,41] For consistency with the previous work of Hassanali et al. on the recombination of the hydronium and hydroxide ions,[38] the exchange-correlation interaction was described using the PBE functional.[42] Of course, the sensitivity of AIMD simulation with respect to the choice of the density functional is always a concern, in particular for aqueous systems.[14,43−48] Indeed, many popular and widely used generalized gradient approximated (GGA) functionals such as PBE[42] or BLYP[49,50] have been shown to

dx.doi.org/10.1021/jp507246e | J. Phys. Chem. B 2014, 118, 13903−13912

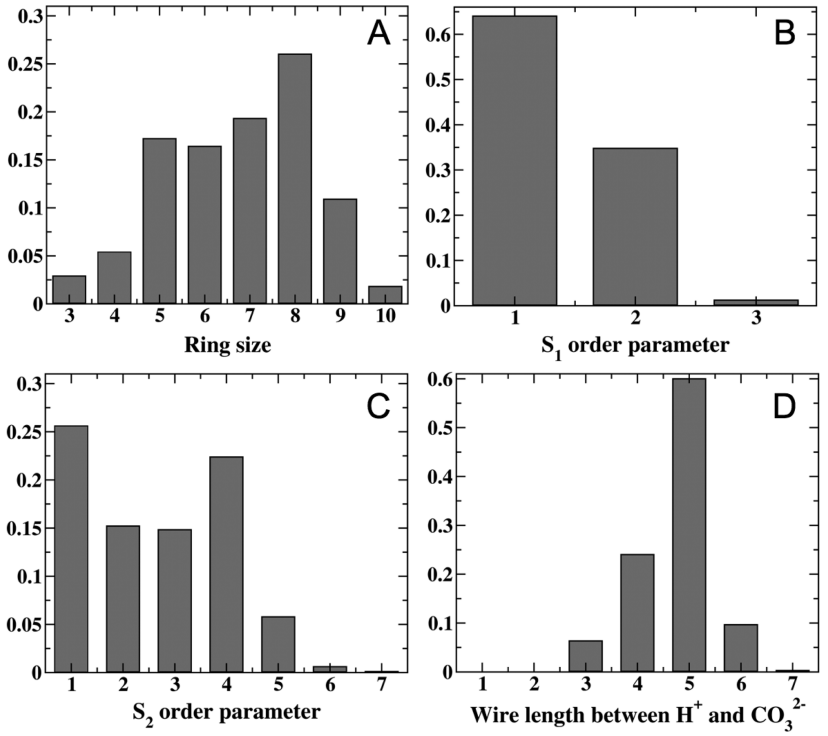

Figure 2. (A) Distribution of the size of the rings threading the carbonate ion obtained from the $t = 0$ frame of all of the recombination trajectories performed at 300 K. Distribution of the S_1 (B) and S_2 (C) order parameters characteristic of these rings. (D) Distribution of the length of shortest path between the proton and the three oxygen atoms of the carbonate at the beginning of the recombination trajectories. For 2% of the frames, the two ions are initially not linked by a directed water wire.

lead to an overstructured liquid water compared to experiments. Thus, to ascertain the validity of our results with respect to our choice of the PBE functional, we have repeated our calculations at 300 K using the HCTH/120 functional.[51] This functional, although also belonging to the GGA-type of functionals, has been shown to be particularly better for hydrogen-bonded systems and also to yield a less structured liquid water.[9,46,47] Hence, it represents a good test of the accuracy of our results. Furthermore, we also performed, at 300 K, calculations including empirical corrections to the PBE functional to take into account the dispersion interactions that are poorly described by GGA functionals.[52] These various tests on the validity of our results with respect to the functional are presented in Supporting Information and are discussed below in the text. Another issue of concern that has been raised in the literature with regard to using GGA functionals is the role of the self-interaction error, which can cause spurious charge delocalizations.[53] One illustration is a recent work by Galli and co-workers on the structural and electronic properties of NaCl in aqueous solution that has shown that if one is interested in calculating electronic properties such as the band gap then the use of hybrid functionals such as PBE0[54] is better than PBE, although this is still only in qualitative agreement with experiments.[55] Repeating all of our calculations with hybrid functionals is beyond the scope of the current study, as it would require a very large amount of computational time. However, to assess that we do not have unrealistic charge transfer from CO_3^{2-} to the surrounding water molecules, we compared the electronic density of the highest occupied Kohn−Sham molecular orbital calculated using PBE and the hybrid functional PBE0 for one frame for which recombination has not occurred. As presented in the Supporting Information, the difference in electronic density calculated with the two functionals is very small. Thus, this gives us confidence that our simulations are hardly subject to the aforementioned spurious charge delocalizations.

Energy cutoff of 40 and 320 Ry were used to describe the wave functions and the electronic density, respectively, in combination with ultrasoft pseudopotentials[56] to treat the ion−electron interaction. A Γ-point sampling of the first Brillouin zone was performed. We used a fictitious electron mass of 350 a.u., and the nuclei were propagated classically using a time step of 0.125 fs. All hydrogen atoms were assigned the mass of the deuterium to allow for a larger time step in the CPMD simulations. It is worth noting that most of the experimental studies that we have referred to in the Introduction have been conducted on fully deuterated systems, thus reinforcing this choice and allowing for a more meaningful comparison with the experiments. For all of the calculations performed in the canonical ensemble, a thermostat based on a colored-noise generalized Langevin equation was used.[57]

Analysis of the Trajectories. An essential requirement to analyze the recombination events involves being able to track the various protons being transferred along the simulations. To do so, we first determined the trajectories that led to an effective recombination by identifying, from the final frames of each simulation, those that had a hydrogen atom that was covalently linked to a carbonate oxygen. This was achieved using a geometric criterion, namely, when the O−H distance was less than 1.05 Å. Once such a trajectory is identified, we then looked for the oxygen atom that donated this proton. This was determined by finding the oxygen where the O−H distance of the transferred proton was less than or equal to 1.05 Å. This back-trace process is then repeated for the two hydrogen atoms

dx.doi.org/10.1021/jp507246e | J. Phys. Chem. B 2014, 118, 13903−13912

linked to this oxygen, among which only one is transferred, until we reached the initially known hydronium oxygen atom.

RESULTS AND DISCUSSION

The mechanisms for acid−base recombination described in the Introduction are part of a more general chemical equilibrium scheme that was described by Eigen.[18] This scheme is composed of three branches, namely, hydrolysis, direct proton exchange, and protolysis pathways.[27] The first one corresponds to the hydrolysis of the base associated with the formation of a hydroxide ion that subsequently diffuses in solution and neutralizes the acid. The second occurs when a close contact between the acid and the base exists and prevents the diffusion of ionic species in solution. Finally, the protolysis mechanism results from the dissociation of the acid with the diffusion of the proton in solution. Each pathway is characterized by specific time scales, and their ratio depends sensitively on the experimental conditions. In particular, the concentration of the solutes play an important role in determining the ratio between the direct proton exchange and the protolysis routes. From the point of view of AIMD, it is computationally prohibitive to probe and characterize the role of each of these pathways because it would require large system sizes and long simulation times. Consequently, we have restricted ourself to study the protolysis pathway, i.e., we studied the recombination between a base and a single proton diffusing in the solvent without any effect of the initial conditions that have generated this proton, for example, the excitation of the photoacid. Experimentally, this would correspond to a solution with a low base concentration. We have chosen as model base the carbonate ion CO_3^{2-}, as it is a common weak base that is chemically quite similar to the experimentally studied acetates and that is computationally tractable due to its small size.

H_3O^+ and CO_3^{2-} Hydrogen-Bond Network. In a recent work, by examining topological relationships of closed directed rings, we have shown that water's hydrogen-bond network is characterized by medium-range directional correlations.[16] This property results in the presence of proton wires around the hydronium and hydroxide ions that serve as conduits for longer-range PTs than previously anticipated. Thus, a first question that naturally follows within the context of the present work is the nature of the directed rings that decorate the carbonate and that potentially connect it to the hydronium ion. To answer this question, we analyzed the distribution of the size of the rings threading at least one of the oxygen atoms of the carbonate as well as the distribution of the S_1 and S_2 parameters, introduced in our earlier study,[16] characteristic of these rings.

We briefly recall that S_1 measures the number of donor−donor (DD) and acceptor−acceptor (AA) water molecules within the ring, whereas S_2 is a measure of the longest directed path that can occur along the ring. The results are displayed in Figure 2 for the initial configuration of all of the recombination trajectories performed at 300 K. The size of the rings (Figure 2A) ranges between 3 and 10 but is dominated by five- to eight-membered rings. As far as the directionality within the rings is concerned, as probed by S_1, we see that the S_1 distribution (Figure 2B) is quite similar to the one observed in pure liquid water.[16] In our case, the one important difference is that no $S_1 = 0$ ring is observed because the carbonate oxygens always play the role of AA.

The S_2 order parameter shown in Figure 2C probes the diversity of sequential directed hydrogen bonds that could potentially act as pathways through which the proton can hop. Depending on the size of the ring and its value of S_1, we observe quite a broad distribution ranging from 1 to 7. S_2 focuses exclusively on pathways within the ring. Upon inspecting our trajectories, we found that, in many cases, H_3O^+ did not necessarily participate within the same closed ring as the oxygens of the carbonate. Hence, the S_2 parameter does not directly capture a directed path from the hydronium to the carbonate. To probe the presence of longer-range pathways across different rings, we examined the distribution of shortest directed paths from the hydronium to any of the three carbonate oxygens, which is illustrated in Figure 2D. As can be seen, there is a broad distribution of directed pathways from H_3O^+ to the carbonate, implying that a large variety of potential reactive complex structures are visited at the beginning of our trajectories, of which four are displayed in Figure 3. A closer

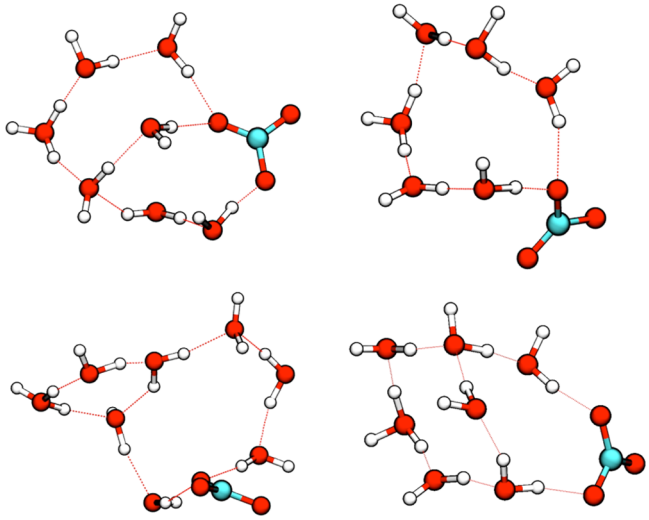

Figure 3. Four examples of the structure of the reactive complex at the beginning of the energy-conserving simulations ($t = 0$) at 300 K. Each snapshot represents the CO_3^{2-} and H_3O^+ ions and a nonexhaustive number of water wires linking them.

look at these distributions reveals that, except for a small proportion of the simulations where CO_3^{2-} and H_3O^+ are initially not linked together (2% in Figure 2D), proton wires of length varying between 3 and 7 always link the two charged species. Consequently, we observed in our simulations that the number of water molecules implied in the neutralization, i.e., carrying the excess proton at any moment during the simulation, can vary from three, in the recombinations that occur along water wires containing two water molecules, or more if the proton does not take the shortest pathway toward the base. As these latter are rarer events, we have focused the ensuing analysis on the three last PTs occurring before neutralization.

Within the limits of our approximations, the simulations at 300 and 400 K yield quite similar ring and wire distributions (see Supporting Information for the data at 400 K), suggesting that the underlying mechanisms in this temperature range would be quite similar once the ions have reached contact distance. However, it is clear that an important part of the mechanism that is missing from our current study is the transition from the diffusive regime to this contact distance. Indeed, the dynamics of this process would certainly be strongly sensitive to the reorganization of the hydrogen-bond

dx.doi.org/10.1021/jp507246e | J. Phys. Chem. B 2014, 118, 13903−13912

network sandwiched between the two approaching species, which is statistically poorly explored by our simulations, mainly because of the short simulation times and finite box size effects. However, this part of the process is beyond the scope of the current study and hence we focus now on the mechanisms occurring once the ions have already reached contact distance.

Recombination Mechanism at 300 and 400 K. In the previous section, we have established the existence of medium-to-long-range hydrogen bond wires that serve as potential pathways for proton recombination with the carbonate ion. We now focus our study on the structural and dynamical processes involved in this process.

Concerted Character of the Recombination. To characterize the recombination, we defined the so-called proton transfer coordinates, $\nu(i)$ (i = 1, 2, and 3; Figure 1), associated with the ith proton along the wire and defined by $\nu(i) = r_{O(i+1)-H(i)} - r_{H(i)-O(i)}$. O(1) is the carbonate oxygen, and H(1) is the proton that recombines with it. When a proton is transferred between two water molecules, it passes through $\nu(i) = 0$. To examine the relative degree of stepwise and concerted PT along the wires, we analyzed the correlations that exist between their respective ν. Figure 4 presents the three density plots obtained for $\nu(1)/\nu(2)$, $\nu(2)/\nu(3)$, and $\nu(1)/\nu(3)$ obtained from all of the recombination events observed at 300 K. From our definition of $\nu(i)$, the {−1;−1} and {1;1} basins represent the initial and final configurations, respectively. As can be seen in Figure 4A, the transfer of the two protons closer to the carbonate, associated with $\nu(1)$ and $\nu(2)$, are highly correlated, as the intermediate configurations are located close to the {0;0} state and no basin is observed in this region. Thus, a contact ion pair CO_3^{2-}−H_3O^+ does not form in this case. As one examines the correlation between the other PTs, the extent of the concertedness gets weaker, but it is not entirely lost. For example, the distribution depicted in Figure 4B has less propensity along the diagonal, revealing a less pronounced concerted motion between H(2) and H(3). Of course, this weaker concerted behavior between H(2) and H(3) is even more pronounced for the PTs associated with H(1) and H(3), as seen in Figure 4C.

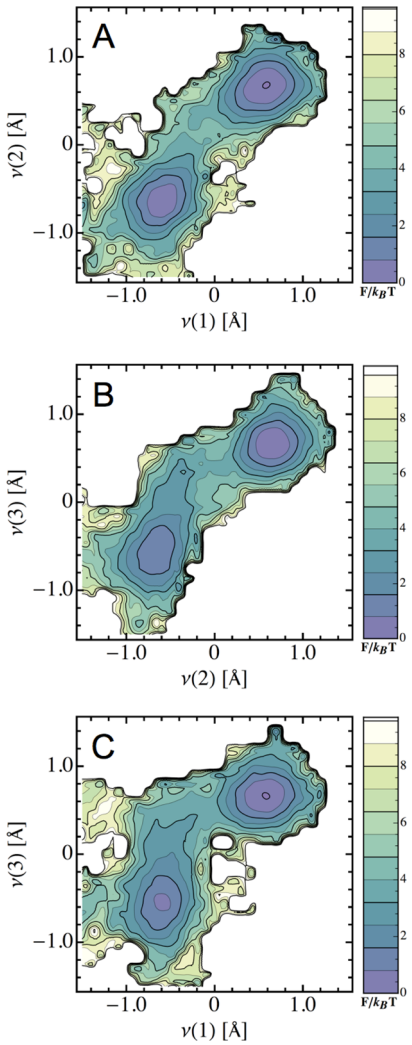

Figure 4. Density plots of ν_1/ν_2 (A), ν_2/ν_3 (B), and ν_1/ν_3 (C) obtained from all of the recombination observed at 300 K.

Collective Wire Compression. In their pioneering work on PT in bulk water, Marx et al. demonstrated that the compression of the oxygen atoms sandwiching the proton is an important parameter for facilitating PT between two water molecules.[7] Within the framework of the recombination of hydroxide and hydronium, as well as in the motion of the isolated proton in the bulk, Hassanali and co-workers have recently found that the phenomena of collective compression can be longer range.[16,38] In particular, collective modes of water wires can lead to concerted PTs over several water molecules. Thus, our previous observations involving concerted PTs during the recombination of CO_3^{2-} with a proton suggest that this feature is likely to be occurring here as well. Figure 5A shows the correlation between $\nu(1)$ and the $r_{O(1)-O(2)}$ distance (in the Supporting Information, similar plots are presented for H(2) and H(3)). It is clear from these pictures that the PT is strongly coupled to the compression of the two surrounding oxygen atoms, i.e., of the surrounding water molecules. More

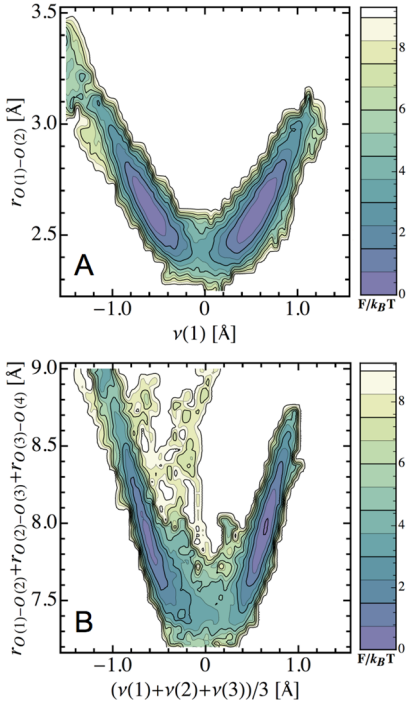

Figure 5. Density plots obtained for $r_{O(1)-O(2)}$ vs $\nu(1)$ (A) and $(r_{O(1)-O(2)} + r_{O(2)-O(3)} + r_{O(3)-O(4)})$ vs $(\nu(1) + \nu(2) + \nu(3))/3$ (B) obtained from all of the recombinations observed at 300 K.

dx.doi.org/10.1021/jp507246e | J. Phys. Chem. B 2014, 118, 13903−13912

importantly and similar to earlier work, this correlation not only exists for a single proton but also has a more extended character along the water wire. Figure 5B highlights this observation by displaying the correlation between the average ν and the sum of the three oxygen−oxygen distances along the wire. As already shown by Figure 4B, the small buildup of population observed in Figure 5B for ν between −0.2 and −0.6 Å is due to the weaker concertedness of H(2) and H(3) compared to that of H(1) and H(2).

Mechanism at 300 K and Discussion. These results suggest that the recombination occurs in two steps: first, a weakly concerted PT leads to the formation of a tight reactive complex containing only one bridging water, and then two PTs occur in a strongly concerted fashion. To illustrate the extent of the concertedness, we have defined for each PT its proton transfer time in the following manner: in our back-trace process described earlier, the PT time is defined as the instant when the transferred proton first reaches a distance longer than 1.05 Å with the oxygen to which it is bound. Figure 6 displays the PT

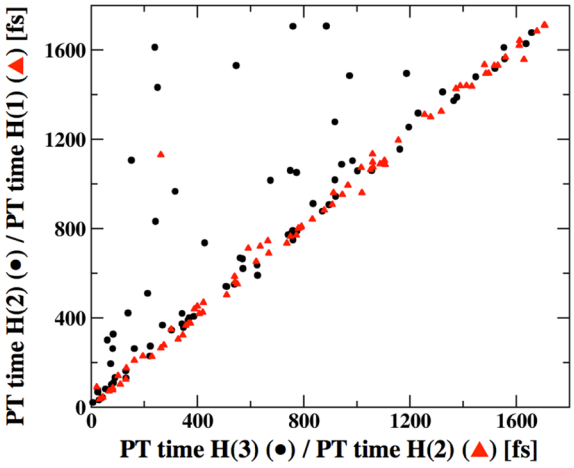

Figure 6. Proton transfer time of H(2) vs proton transfer time of H(3) (black circle) and proton transfer time of H(1) vs proton transfer time of H(2) (red triangle) for each trajectory performed at 300 K. See text for the definition of the proton transfer times.

time of H(1) versus H(2) and H(2) versus H(3). To draw this picture with a sufficient number of points, we included all of the data available from the two sets of simulations performed at 300 K. As can be seen, the PT transfer times of H(1) and H(2) are identical in the large majority of the trajectories and thus fall on a line with slope close to 1. In contrast, the PT transfer times of H(2) display a relatively larger lag with the ones of H(3), which is consistent with the weaker concerted character observed on Figure 4B.

It is interesting to compare our current results with those obtained from the recombination of the hydronium and hydroxide where a concerted jump of three protons was observed.[38] Understanding the exact origin of these differences is not trivial, but we can speculate on some of the factors that control this process. The first is related to the nature of the electronic interactions between the ions. For the hydronium−hydroxide system, this involves a mixture of electrostatic, polarization, and charge transfer effects, as both the proton and hydroxide are fluxional entities that can delocalize across the hydrogen-bond network. In contrast, in the case of CO_3^{2-}, the interaction is dominated by electrostatics and is likely to be weaker than the compounded interactions in the hydronium−hydroxide system. A second argument is that, although both CO_3^{2-} and OH^- alter the local vibrational modes of water, CO_3^{2-} is a larger entity, which may decrease its ability to funnel vibrational energy into collective vibrational modes compared to that of the hydroxide ion.

At this juncture, we would like to recall that our simulations focus on the protolysis mechanism of acid−base recombination, although this is not the only one occurring in solution. It is thus useful to compare and discuss the mechanisms that we observe to those of other theoretical studies performed on other chemical systems using different computational methods. These simulations fall in to two main classes: first, those that look at the recombination of an acid and a base as we do, and, second, studies that look at the time-reversed process, namely, the deprotonation of an acid.

Thomas et al. recently published a study in which they have simulated the neutralization of a phenolic derivative and the formate ion.[58] In this work, the authors focused their analysis on the direct proton exchange mechanism in which the phenolic derivative and the formate ion are separated by a single water molecule, with their relative distance being restrained. By using a dipole-field/quantum mechanics model to control the pK_a of their system, they were able to induce several deprotonation and protonation events of the acid and base, respectively. Their simulations displayed two different transfer mechanisms: one sequential, which is largely predominant, with the formation of a long-lived intermediate, and one concerted. This apparent difference in the extent of concerted PT between this study and ours underlines the sensitivity of the PT mechanism to the physicochemical conditions of the reaction. Since the contact ion pair formed between the phenolic/formate pair is less flexible, the collective compression required for a concerted jump is less likely to occur. We can, however, anticipate that the same simulation performed with two bridging water molecules could possibly enhance the extent of concerted PT events.

The time-reversed process for recombination beyond contact distance is typically an activated process that cannot be simulated on the time scales of current AIMD simulations and hence requires some form of enhanced sampling simulation methods. Park et al. studied the deprotonation of acetic acid by combining metadynamics[59−61] and transition path sampling (TPS)[62] simulations.[63] Although they studied a chemically different system, the qualitative picture that they were able to extract from their simulations displays some common features with our results. Indeed, among the 21 transition paths that they gathered for which deprotonation occurs, half of them were characterized by a metastable contact ion pair intermediate. To occur, this mechanism was shown to require significant solvent reorganization around the proton-accepting water molecule and the hydroxyl oxygen atom. In the other half of the transition paths, no contact ion pair was observed, and a concerted motion of two protons was evidenced that was further followed by subsequent PTs in the solvent. Although the authors did not report a water wire compression during the deprotonation, this second mechanism is quite similar to what we observe for the protonation mechanism of CO_3^{2-}. The fact that our simulations do not display any contact ion pair intermediate, i.e., a CO_3^{2-}−H_3O^+ complex that exists for several tens of femtoseconds, might seem surprising. However, one has to keep in mind the difference of pK_a between the two acids HCO_3^- (10.33) and CH_3COOH (4.70), which shows that there is a stronger driving force for CO_3^{2-} to accept a proton than for

dx.doi.org/10.1021/jp507246e | J. Phys. Chem. B 2014, 118, 13903−13912

CH_3COO^-. The absence of contact ion pairs in our simulations can thus be attributed to the higher affinity of CO_3^{2-} for the excess proton. In Figure 6, one can see one point (at the position {262.5;1130.0}) for which there is a significant difference between the PT times of H(1) and H(2). Although this data could suggest the existence of contact a ion pair, a visual inspection of this particular trajectory reveals that the water molecule receiving H(2) is at a distance of ∼4 Å from the carbonate ion at the PT time. Thus, a significant amount of time is needed to bring the newly formed H_3O^+ in contact with CO_3^{2-}. As soon as this contact is formed, the PT is instantaneous.

Another important work that holds connections with our current work is the study by Geissler et al. on the autoionization of liquid water, i.e., the time-reversed process for the hydronium−hydroxide recombination.[64] By combining AIMD and TPS simulations, the authors demonstrated the fundamental role of electric field fluctuations in the process. In these studies, the breakage of a hydrogen-bond wire linking the ions was found to be a critical part to ensure that the ions do not recombine. Later studies by Eaves et al. examined how electric field fluctuations drove vibrational dephasing and found some interesting correlations between the frequency of the O−H stretching mode and the electric field along the hydrogen bonds as well as the extent of the compression of the hydrogen bond.[65] More recently, Reischl et al. have found that the strength of the electric field along the O−H bonds in liquid water is caused mostly by waters in the immediate solvation shell.[66] Within the context of our current work, we find that the percolating network between the CO_3^{2-} and the excess proton results in a broad distribution of wires that bridge the two species and that their compression is critical for ensuring recombination. As in the recombination of hydronium and hydroxide, the wire is a necessary but not sufficient condition for inducing recombination. Given the correlations revealed by Eaves et al. between the electric field fluctuations, the O−H stretch frequency, and the O−O bond length, the collective compressions that we observed might certainly have correlations with such electric field fluctuations.

Role of Finite Temperature. As alluded to earlier in the article, to assess the role of finite temperature on the recombination mechanism, we performed a similar study at 400 K. Experimentally, Cox et al. have demonstrated that, for the recombination of a photoacid and the acetate ion, an increase of the temperature by several tens of degrees results in a decrease of the transfer rate.[33] This was interpreted as originating from the disruption of proton wires that are an essential ingredient for concerted proton hopping. Surprisingly, our results shown in Figure 7 are quite similar to those in Figure 4. This demonstrates that at higher temperature the concerted PT mechanism is not shut off. This comes from the fact that while the lifetime of the rings and wires threading the carbonate certainly decrease at higher temperatures their architectures still remain and hence provide the pathways for long-range proton hopping.

One can wonder why our simulations do not show a net difference in the ability of protons to undergo concerted PTs. Perhaps one of the most important factors concerns the choice of the initial conditions established by the finite size of the box, where the proton and carbonate are already at contact distance. An important component of the recombination mechanism involves the transition from the diffusive regime to that of contact distance, and this is a feature that we do not capture in our current simulations. This part of the process would be affected by the change of temperature and thus the global temperature dependence observed Figure 8 of the paper by Cox et al. do not necessarily arise from what happens at contact distance. Another important factor is the level of accuracy of the potential energy surface that we explore. Indeed, as alluded to earlier in the text, it is well-appreciated that standard DFT functionals tend to overstructure liquid water, leading to stronger hydrogen bonds between water molecules.[14,43−48] The origins of this discrepancy is an ongoing topic of research and has been attributed to the fact that AIMD simulations based on GGA functionals do not treat dispersion[67] and exact exchange[68] and also do not include nuclear quantum effects, which have been shown to significantly enhance the delocalization of the proton along the hydrogen bonds in liquid water.[69,70] However, it was shown in the earlier studies of the recombination of hydronium and hydroxide that the qualitative trends of the observed mechanism are not sensitive to the choice of the GGA functional.[38] To confirm that this observation is also valid for our system, we performed simulations at 300 K using the HCTH/120 functional that has been shown by several works to lead to a less frozen liquid than that with PBE and BLYP.[9,46,47] The corresponding results are presented in the Supporting Informations and show that all aspects of the mechanism that we propose stay qualitatively the same. We also performed simulations using the PBE-D functional, for which empirical corrections that take into account the dispersion interactions are added to the PBE functional (see Supporting Informations). Here again, the key results, namely, the presence of correlated proton hopping, collective compressions, and the solvent reorganization (see below), are qualitatively the same. Consequently, these tests give us confidence in the mechanisms that we have found for the recombination of the proton with the carbonate anion.

Thus, we reiterate that what can be inferred from our simulations is that when the ions reach contact distance

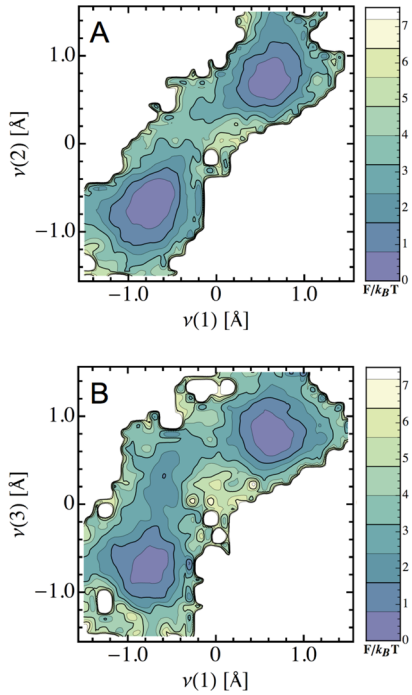

Figure 7. Density plots of ν_1/ν_2 (A) and ν_1/ν_3 (B) obtained from all of the recombination observed at 400 K.

dx.doi.org/10.1021/jp507246e | J. Phys. Chem. B 2014, 118, 13903−13912

concerted PT appears to occur at both low and high temperatures. Thus, one can expect that at the higher temperatures the rate-limiting step of recombination will be controlled by bringing the ions to contact distance, i.e., the network reorganization required to form the loose complex proposed by Rini et al. However, accurately describing this aspect of the recombination mechanism would require the simulation of larger systems and, more importantly, a much finer statistical convergence of the data.

Solvent Reorganization. The structural and dynamical properties of the hydration shell of CO_3^{2-} have been extensively studied by Bruneval et al. using an empirical force field.[71] In their simulations, the authors evidenced a strong interaction of CO_3^{2-} with the solvent water molecules, which is revealed by quite a long residence time of ~36 ± 6 ps, indicating that the waters are strongly bound to the anionic species. Despite this strong interaction, the average number of hydrogen bonds per oxygen that they obtained (~4.03) obviously varies due to local density fluctuations in the solvent. As shown earlier in the text, the CO_3^{2-} anion is threaded by a distribution of directed rings, the structure of which is important for concerted PTs events that are also affected by local fluctuations of the hydration shell. Since these fluctuations are already known to play an important role in PT in neat liquid water,[16] we were thus interested in assessing the structural and dynamical behavior of the first hydration shell of the carbonate prior to and after the recombination events.

Figure 8A shows the distribution of the total number of hydrogen and covalent bonds between the oxygen atom that gets protonated and the hydrogen atoms of the system as a function of $\nu(1)$. Before recombination, this number ranges between 2 and 4. The horizontal channels along $\nu(1)$ clearly show that only the oxygen atoms with coordination numbers between 2 and 3 are susceptible to be protonated. In fact, when the carbonate oxygen accepts four hydrogen bonds, we do not see any protonation events. Within the limits of our statistics, we find that ~75% of the recombination trajectories go through structures that have initially a coordination number of 2. Although our recombination trajectories are limited to 2 ps, this delay allows us to observe a modification of the first hydration shell of the protonated oxygen, which clearly shows a tendency to lose hydrogen bonds. These results are consistent with the AIMD simulations of Kumar and co-workers who showed that the OH of HCO_3^- accepts, on average, less than two hydrogen bonds compared to an oxygen atom of CO_3^{2-}.[72] Furthermore, we also see that the last PT given by $\nu(1)$ and the solvent fluctuations, as probed by CN_{CO-H}, occur predominantly in a stepwise manner. In other words, it involves a larger barrier to reorganize both $\nu(1)$ and CN_{CO-H} in a concerted manner rather than reorganizing the hydration shell once recombination occurs.

Besides the changes in solvation at the site being protonated, there are also some changes at the two carbonate oxygens that do not get protonated. This is illustrated in Figure 8B, which shows the distribution of the sum of the number of hydrogen bonds between these two oxygen atoms and all of the hydrogen atoms of the system as a function of $\nu(1)$. Before recombination, and in the limit of the statistical convergence of our simulations, they display a rather similar hydration shell compared to the recombining oxygen. Indeed, the predominance of the coordination numbers of 2−3 per carbonate oxygen atom leads to values of 5−6 in Figure 8B, and the occasional appearance of a four coordinated oxygen leads to a

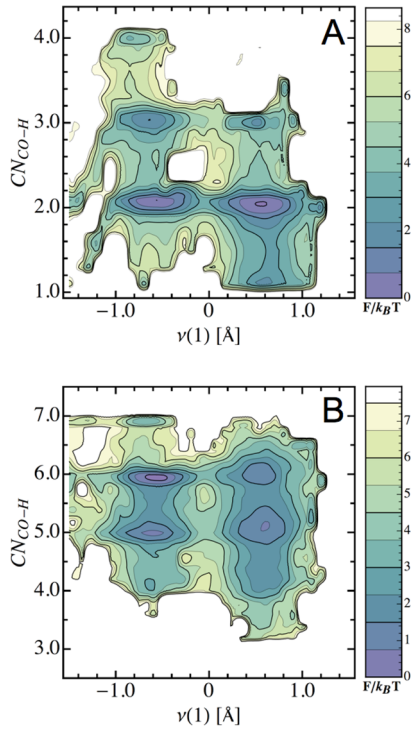

Figure 8. (A) Density plot illustrating the correlation between $\nu(1)$ and the coordination number of the protonated oxygen atom of CO_3^{2-} with all the surrounding hydrogen atoms for the recombination trajectories at 300 K. (B) Similar plot for the sum of the coordination numbers of the two nonprotonated oxygen atoms of CO_3^{2-}. The coordination numbers are equal to 1 when $r_{O-H} \leq 1.8$ Å and to the following switching function: $(1-(r_{O-H} - 1.8/0.4)^6)/(r_{O-H} - 1.8/0.4)^{12})$ when $r_{O-H} > 1.8$ Å.

value of 7. In the current simulations, we do not sample any configuration where the two oxygens that do not recombine with the proton are each hydrogen-bonded to four water molecules. The similarity in the hydration environment of both the oxygen getting protonated and those that do not shows that the recombination process is not driven by any asymmetries in the hydration structure at different base sites. Rather, it appears to be more strongly coupled to the ability of the proton to form a reactive tight complex with the carbonate, which is probably driven by the network fluctuations around the proton. Similar to the carbonate oxygen getting protonated, the recombination also leads to a shift in the distribution of the CN_{CO-H} distribution to lower values for those that remain unprotonated. Thus, the recombination mechanism involves a collective reorganization of the water network around the CO_3^{2-} that occurs on the picosecond time scale after recombination.

■ CONCLUSIONS

In this article, we have examined the molecular mechanism associated with the recombination of a proton with a weak Brønsted base. Our simulations suggest that once a reactive complex with two bridging water molecules is formed between CO_3^{2-} and H_3O^+ the acid−base recombination occurs mainly through concerted hopping of protons over several hydrogen bonds. In contrast to the hydronium−hydroxide recombination, the first of these three transfers is more decoupled from the other two PT events. Furthermore, the concerted events that we observe are clearly facilitated by global compressions of the water wires, which corroborates the conclusions made by

dx.doi.org/10.1021/jp507246e | J. Phys. Chem. B 2014, 118, 13903−13912

Hassanali et al. on the key role of this compression for the neutralization of the hydroxide and hydronium ions.[38] Finally, the ability of an oxygen atom to be protonated appears to be quite sensitive to its hydration structure, with the latter being drastically modified after the recombination. It is worth pointing out that despite the challenges of DFT to quantitatively describe the structure of liquid water we have shown in previous studies that the qualitative insights into the mechanisms of proton transfer are not sensitive to the choice of the exchange-correlation functional.[16,38] It is, however, expected that the inclusion of nuclear quantum effects will likely play a critical role in tuning the ratio of concerted and stepwise transfers along the water wires.[70] Thus, examining the role of nuclear quantum effects on this process would be an interesting topic to pursue in the future.

■ ASSOCIATED CONTENT

Supporting Information

Description of the hydrogen-bond network around H_3O^+ and CO_3^{2-} described in terms of ring statistics at 400 K and the $\nu(2)/r_{O(2)-O(3)}$ and $\nu(3)/r_{O(3)-O(4)}$ correlations obtained at 300 K using the PBE functional. Also provided are plots of the data of the second set of simulations at both 300 and 400 K and performed using the PBE functional. We also provide results obtained from the data of simulations performed using the HCTH/120 and PBE-D functionals at 300 K. Finally, a calculation performed with the PBE0 functional is presented to demonstrate that our calculations are not subject to spurious charge delocalization. This material is available free of charge via the Internet at http://pubs.acs.org.

■ AUTHOR INFORMATION

Corresponding Authors

*(J.C.) E-mail: jerome.cuny@irsamc.ups-tlse.fr. Phone: +33 (0) 561556836. Fax: +33 (0) 561556065.

*(A.A.H.) E-mail: ahassana@ictp.it.

Notes

The authors declare no competing financial interest.

■ ACKNOWLEDGMENTS

The authors thank generous allocations of computer time from the Swiss National Computing Center (Project s312) and the University of Lugano. The authors also thank the supercomputing facility of Toulouse III University, CALMIP, for allocation of computer resources (Project P1320).

■ REFERENCES

(1) Kühlbrandt, W. Bacteriorhodopsin—the Movie. *Nature* **2000**, *406*, 569−570.

(2) Ball, P. Water as an Active Constituent in Cell Biology. *Chem. Rev.* **2007**, *108*, 74−108.

(3) Freier, E.; Wolf, S.; Gerwert, K. Proton Transfer via a Transient Linear Water-Molecule Chain in a Membrane Protein. *Proc. Natl. Acad. Sci. U.S.A.* **2011**, *108*, 11435−11439.

(4) Huber, G. W.; Iborra, S.; Corma, A. Synthesis of Transportation Fuels from Biomass: Chemistry, Catalysts, and Engineering. *Chem. Rev.* **2006**, *106*, 4044−4098.

(5) Tuckerman, M.; Laasonen, K.; Sprik, M.; Parrinello, M. Ab Initio Molecular Dynamics Simulation of the Solvation and Transport of H_3O^+ and OH^- Ions in Water. *J. Phys. Chem.* **1995**, *99*, 5749−5752.

(6) Tuckerman, M.; Laasonen, K.; Sprik, M.; Parrinello, M. Ab Initio Molecular Dynamics Simulation of the Solvation and Transport of Hydronium and Hydroxyl Ions in Water. *J. Chem. Phys.* **1995**, *103*, 150−161.

(7) Marx, D.; Tuckerman, M. E.; Hutter, J.; Parrinello, M. The Nature of the Hydrated Excess Proton in Water. *Nature* **1999**, *397*, 601−604.

(8) Chandra, A.; Tuckerman, M. E.; Marx, D. Connecting Solvation Shell Structure to Proton Transport Kinetics in Hydrogen-Bonded Networks via Population Correlation Functions. *Phys. Rev. Lett.* **2007**, *99*, 145901.

(9) Markovitch, O.; Chen, H.; Izvekov, S.; Paesani, F.; Voth, G. A.; Agmon, N. Special Pair Dance and Partner Selection: Elementary Steps in Proton Transport in Liquid Water. *J. Phys. Chem. B* **2008**, *112*, 9456−9466.

(10) Berkelbach, T. C.; Lee, H.-S.; Tuckerman, M. E. Concerted Hydrogen-Bond Dynamics in the Transport Mechanism of the Hydrated Proton: A First-Principles Molecular Dynamics Study. *Phys. Rev. Lett.* **2009**, *103*, 238302.

(11) Swanson, J. M. J.; Simons, J. Role of Charge Transfer in the Structure and Dynamics of the Hydrated Proton. *J. Phys. Chem. B* **2009**, *113*, 5149−5161.

(12) Knight, C.; Maupin, C. M.; Izvekov, S.; Voth, G. A. Defining Condensed Phase Reactive Force Fields from Ab-Initio Molecular Dynamics Simulations: The Case of the Hydrated Excess Proton. *J. Chem. Theory Comput.* **2010**, *6*, 3223−3232.

(13) Knight, C.; Voth, G. A. The Curious Case of the Hydrated Proton. *Acc. Chem. Res.* **2012**, *45*, 101−109.

(14) Hassanali, A. A.; Cuny, J.; Verdolino, V.; Parrinello, M. Aqueous Solutions: State of the Art in Ab Initio Molecular Dynamics. *Philos. Trans. R. Soc. A* **2014**, *372*, 20120482.

(15) de Grotthuss, C. J. T. Mémoire sur la Décomposition de l'Eau et des Corps Qu'elle Tient en Dissolution à l'Aide de l'Électricité Galvanique. *Ann. Chim.* **1806**, *LVIII*, 54−74.

(16) Hassanali, A.; Giberti, F.; Cuny, J.; Kühne, T. D.; Parrinello, M. Proton Transfer Through the Water Gossamer. *Proc. Natl. Acad. Sci. U.S.A.* **2013**, *110*, 13723−13728.

(17) Eigen, M.; Kruse, W.; Maass, G.; De Maeyer, L. Rate Constants of Protolytic Reactions in Aqueous Solution. *Prog. React. Kinet.* **1964**, *2*, 285−318.

(18) Eigen, M. Proton Transfer, Acid-Base Catalysis, and Enzymatic Hydrolysis. Part I: Elementary Processes. *Angew. Chem., Int. Ed. Engl.* **1964**, *3*, 1−19.

(19) Weller, A. Allgemeine Basenkatalyse bei der Elektrolytischen Dissoziation Angeregter Naphthole. *Z. Elektrochem.* **1954**, *58*, 849−853.

(20) Weller, A. Allgemeine Basenkatalyse bei der Elektrolytischen Dissoziation Angeregter Naphthole. *Z. Phys. Chem.* **1958**, *17*, 224−245.

(21) Weller, A. Fast Reactions of Excited Molecules. *Prog. React. Kinet.* **1961**, *1*, 187−214.

(22) Eigen, M.; de Maeyer, L. Self-Dissociation and Protonic Charge Transport in Water and Ice. *Proc. R. Soc. London A* **1958**, *247*, 505−533.

(23) Rini, M.; Magnes, B.-Z.; Pines, E.; Nibbering, E. T. J. Real-Time Observation of Bimodal Proton Transfer in Acid-Base Pairs in Water. *Science* **2003**, *301*, 349−352.

(24) Rini, M.; Pines, D.; Magnes, B.-Z.; Pines, E.; Nibbering, E. T. J. Bimodal Proton Transfer in Acid−Base Reactions in Water. *J. Chem. Phys.* **2004**, *121*, 9593−9610.

(25) Nibbering, E. T.; Fidder, H.; Pines, E. Ultrafast Chemistry: Using Time-Resolved Vibrational Spectroscopy for Interrogation of Structural Dynamics. *Annu. Rev. Phys. Chem.* **2005**, *56*, 337−367.

(26) Mohammed, O. F.; Pines, D.; Dreyer, J.; Pines, E.; Nibbering, E. T. J. Sequential Proton Transfer Through Water Bridges in Acid−Base Reactions. *Science* **2005**, *310*, 83−86.

(27) Mohammed, O. F.; Pines, D.; Nibbering, E. T. J.; Pines, E. Base-Induced Solvent Switches in Acid−Base Reactions. *Angew. Chem., Int. Ed.* **2007**, *46*, 1458−1461.

(28) Mohammed, O. F.; Pines, D.; Pines, E.; Nibbering, E. T. J. Aqueous Bimolecular Proton Transfer in Acid−Base Neutralization. *Chem. Phys.* **2007**, *341*, 240−257.

(29) Siwick, B. J.; Bakker, H. J. On the Role of Water in Intermolecular Proton-Transfer Reactions. *J. Am. Chem. Soc.* **2007**, *129*, 13412−13420.
(30) Siwick, B. J.; Cox, M. J.; Bakker, H. J. Long-Range Proton Transfer in Aqueous Acid−Base Reactions. *J. Phys. Chem. B* **2007**, *112*, 378−389.
(31) Adamczyk, K.; Prémont-Schwarz, M.; Pines, D.; Pines, E.; Nibbering, E. T. J. Real-Time Observation of Carbonic Acid Formation in Aqueous Solution. *Science* **2009**, *326*, 1690−1694.
(32) Cox, M. J.; Bakker, H. J. Parallel Proton Transfer Pathways in Aqueous Acid−Base Reactions. *J. Chem. Phys.* **2008**, *128*, 174501−10.
(33) Cox, M. J.; Timmer, R. L. A.; Bakker, H. J.; Park, S.; Agmon, N. Distance-Dependent Proton Transfer along Water Wires Connecting Acid−Base Pairs. *J. Phys. Chem. A* **2009**, *113*, 6599−6606.
(34) Cox, M. J.; Siwick, B. J.; Bakker, H. J. Influence of Ions on Aqueous Acid−Base Reactions. *ChemPhysChem* **2009**, *10*, 236−244.
(35) Cox, M. J.; Bakker, H. J. Femtosecond Study of the Deuteron-Transfer Dynamics of Naphtol Salts in Water. *J. Phys. Chem. A* **2010**, *114*, 10523−10530.
(36) Agmon, N. The Grotthuss Mechanism. *Chem. Phys. Lett.* **1995**, *244*, 456−462.
(37) Marx, D. Proton Transfer 200 Years after von Grotthuss: Insights from Ab Initio Simulations. *ChemPhysChem* **2007**, *8*, 209−210.
(38) Hassanali, A.; Prakash, M. K.; Eshet, H.; Parrinello, M. On the Recombination of Hydronium and Hydroxide Ions in Water. *Proc. Natl. Acad. Sci. U.S.A.* **2011**, *108*, 20410−20415.
(39) Jorgensen, W. L.; Chandrasekhar, J.; Madura, J. D.; Impey, R. W.; Klein, M. L. Comparison of Simple Potential Functions for Simulating Liquid Water. *J. Chem. Phys.* **1983**, *79*, 926−935.
(40) Car, R.; Parrinello, M. Unified Approach for Molecular Dynamics and Density-Functional Theory. *Phys. Rev. Lett.* **1985**, *55*, 2471−2474.
(41) *CPMD*, version 3.15.1; IBM Corp.: Stuttgart, Germany, 1997−2001; http://www.cpmd.org.
(42) Perdew, J. P.; Burke, K.; Ernzerhof, M. Generalized Gradient Approximation Made Simple. *Phys. Rev. Lett.* **1996**, *77*, 3865−3868.
(43) Sprik, M.; Hutter, J.; Parrinello, M. Ab Initio Molecular Dynamics Simulation of Liquid Water: Comparison of Three Gradient-Corrected Density Functionals. *J. Chem. Phys.* **1996**, *105*, 1142−1152.
(44) Grossman, J. C.; Schwegler, E.; Draeger, E. W.; Gygi, F.; Galli, G. Towards an Assessment of the Accuracy of Density Functional Theory for First Principles Simulations of Water. *J. Chem. Phys.* **2004**, *120*, 300−311.
(45) Schwegler, E.; Grossman, J. C.; Gygi, F.; Galli, G. Towards an Assessment of the Accuracy of Density Functional Theory for First Principles Simulations of Water. II. *J. Chem. Phys.* **2004**, *121*, 5400−5409.
(46) VandeVondele, J.; Mohamed, F.; Krack, M.; Hütter, J.; Sprik, M.; Parrinello, M. The Influence of Temperature and Density Functional Models in Ab Initio Molecular Dynamics Simulation of Liquid Water. *J. Chem. Phys.* **2005**, *122*, 014515.
(47) Izvekov, S.; Voth, G. A. Ab Initio Molecular-Dynamics Simulation of Aqueous Proton Solvation and Transport Revisited. *J. Chem. Phys.* **2005**, *123*, 044505.
(48) Marx, D.; Chandra, A.; Tuckerman, M. E. Aqueous Basic Solutions: Hydroxide Solvation, Structural Diffusion, and Comparison to the Hydrated Proton. *Chem. Rev.* **2010**, *110*, 2174−2216.
(49) Becke, A. D. Density-Functional Exchange-Energy Approximation with Correct Asymptotic Behavior. *Phys. Rev. A* **1988**, *38*, 3098−3100.
(50) Lee, C.; Yang, W.; Parr, R. G. Development of the Colle−Salvetti Correlation-Energy Formula into a Functional of the Electron Density. *Phys. Rev. B* **1988**, *37*, 785−789.
(51) Hamprecht, F. A.; Cohen, A. J.; Tozer, D. J.; Handy, N. C. Development and Assessment of New Exchange-Correlation Functionals. *J. Chem. Phys.* **1998**, *109*, 6264−6271.
(52) Grimme, S. Semiempirical GGA-Type Density Functional Constructed With a Long-Range Dispersion Correction. *J. Comput. Chem.* **2006**, *27*, 1787−1799.
(53) Cohen, A. J.; Mori-Sánchez, P.; Yang, W. Insights into Current Limitations of Density Functional Theory. *Science* **2008**, *321*, 792−794.
(54) Adamo, C.; Barone, V. Toward Reliable Density Functional Methods Without Adjustable Parameters: The PBE0Models. *J. Chem. Phys.* **1999**, *110*, 6158−6170.
(55) Gaiduk, A. P.; Zhang, C.; Gygi, F.; Galli, G. Structural and Electronic Properties of Aqueous NaCl Solutions From Ab Initio Molecular Dynamics Simulations with Hybrid Density Functionals. *Chem. Phys. Lett.* **2014**, *604*, 89−96.
(56) Vanderbilt, D. Soft Self-Consistent Pseudopotentials in a Generalized Eigenvalue Formalism. *Phys. Rev. B: Condens. Matter Mater. Phys.* **1990**, *41*, 7892−7895.
(57) Ceriotti, M.; Bussi, G.; Parrinello, M. Langevin Equation with Colored Noise for Constant-Temperature Molecular Dynamics Simulations. *Phys. Rev. Lett.* **2009**, *102*, 020601.
(58) Thomas, V.; Rivard, U.; Maurer, P.; Bruhàcs, A.; Siwick, B. J.; Iftimie, R. Concerted and Sequential Proton Transfer Mechanisms in Water-Separated Acid−Base Encounter Pairs. *J. Phys. Chem. Lett.* **2012**, *3*, 2633−2637.
(59) Laio, A.; Parrinello, M. Escaping Free-Energy Minima. *Proc. Natl. Acad. Sci. U.S.A.* **2002**, *99*, 12562−12566.
(60) Iannuzzi, M.; Laio, A.; Parrinello, M. Efficient Exploration of Reactive Potential Energy Surfaces Using Car−Parrinello Molecular Dynamics. *Phys. Rev. Lett.* **2003**, *90*, 238302.
(61) Laio, A.; Rodriguez-Fortea, A.; Gervasio, F. L.; Ceccarelli, M.; Parrinello, M. Assessing the Accuracy of Metadynamics. *J. Phys. Chem. B* **2005**, *109*, 6714−6721.
(62) Bolhuis, P. G.; Chandler, D.; Dellago, C.; Geissler, P. L. Transition Path Sampling: Throwing Ropes over Rough Mountain Passes, in the Dark. *Annu. Rev. Phys. Chem.* **2002**, *53*, 291−318.
(63) Park, J. M.; Laio, A.; Iannuzzi, M.; Parrinello, M. Dissociation Mechanism of Acetic Acid in Water. *J. Am. Chem. Soc.* **2006**, *128*, 11318−11319.
(64) Geissler, P. L.; Dellago, C.; Chandler, D.; Hutter, J.; Parrinello, M. Autoionization in Liquid Water. *Science* **2001**, *291*, 2121−2124.
(65) Eaves, J. D.; Tokmakoff, A.; Geissler, P. L. Electric Field Fluctuations Drive Vibrational Dephasing in Water. *J. Phys. Chem. A* **2005**, *109*, 9424−9436.
(66) Reischl, B.; Köfinger, J.; Dellago, C. The Statistics of Electric Field Fluctuations in Liquid Water. *Mol. Phys.* **2009**, *107*, 495−502.
(67) Lin, I.-C.; Seitsonen, A. P.; Coutinho-Neto, M. D.; Tavernelli, I.; Rothlisberger, U. Importance of van der Waals Interactions in Liquid Water. *J. Phys. Chem. B* **2009**, *113*, 1127−1131.
(68) Todorova, T.; Seitsonen, A. P.; Hutter, J.; Kuo, I.-F. W.; Mundy, C. J. Molecular Dynamics Simulation of Liquid Water: Hybrid Density Functionals. *J. Phys. Chem. B* **2006**, *110*, 3685−3691.
(69) Morrone, J. A.; Car, R. Nuclear Quantum Effects in Water. *Phys. Rev. Lett.* **2008**, *101*, 017801.
(70) Ceriotti, M.; Cuny, J.; Parrinello, M.; Manolopoulos, D. E. Nuclear Quantum Effects and Hydrogen Bond Fluctuations in Water. *Proc. Natl. Acad. Sci. U.S.A.* **2013**, *110*, 15591−15596.
(71) Bruneval, F.; Donadio, D.; Parrinello, M. Molecular Dynamics Study of the Solvation of Calcium Carbonate in Water. *J. Phys. Chem. B* **2007**, *111*, 12219−12227.
(72) Kumar, P. P.; Kalinichev, A. G.; Kirkpatrick, R. J. Hydrogen-Bonding Structure and Dynamics of Aqueous Carbonate Species from Car−Parrinello Molecular Dynamics Simulations. *J. Phys. Chem. B* **2009**, *113*, 794−802.